

Kinetic investigations of NaF:Cu luminescence

B. Moine and C. Pedrini

Equipe de Recherche Associée No. 1003 Centre National de la Recherche Scientifique, University Claude Bernard Lyon I, 43 Boulevard du 11 Novembre 1918, 69622 Villeurbanne, France

(Received 24 October 1983)

The temperature dependence of the lifetime of Cu^+ impurity ions in single-crystal sodium fluoride has been analyzed. In order to describe the emission process occurring in this system, we have proposed a three-level model including the ground state and two close excited states in thermal equilibrium. Information is deduced concerning mainly their emission probabilities and their energy differences. A calculation of the mixing of these triplet emitting levels with other excited states is in very good agreement with our experimental results.

I. INTRODUCTION

As was done in earlier papers,^{1,2} monovalent copper was successfully introduced into single-crystal sodium fluoride. The optical absorption and emission spectra of this system are actually characteristic of the Cu^+ impurity ions in alkali halides. In particular, the near-ultraviolet absorption bands are assigned to the $3d^{10} \rightarrow 3d^9 4s$ parity-forbidden transition of Cu^+ , made possible by phonon assistance in these centrosymmetric crystals.

Eight states are associated with the excited configuration: 1E_g , $^1T_{2g}$, $^3E_g(T_{1g}, T_{2g})$, and $^3T_{2g}(A_{2g}, E_g, T_{1g}, T_{2g})$. The two-photon polarized spectra lead one to assign the two main absorption bands in the near-uv range to the $^1A_{1g} \rightarrow ^1E_g$ and $^1A_{1g} \rightarrow ^1T_{2g}$ spin-allowed transitions. As is usually the case for Cu^+ in alkali halides, the fluorescent emission, which is observed around 3800 Å in $\text{Cu}^+:\text{NaF}$, is probably the $^3E_g \rightarrow ^1A_{1g}$ spin-forbidden transition. As a result of the spin-orbit coupling, the 3E_g state is split into two close states T_{2g} and T_{1g} , so the emission mechanism should involve these excited states. The emission process of Cu^+ and Ag^+ in other alkali halides have been correctly interpreted by using a three-level model in which the two excited states are close and in thermal equilibrium over a substantial temperature range.³⁻⁶

In this paper, we will show the temperature dependence of the decay times and will use the same model to explain the emission mechanism and to calculate the various parameters which govern it. This model was tested recently by Payne *et al.*⁷ who studied the effect of a magnetic field on the luminescent lifetime of Cu^+ in alkali-halide host crystals. These magnetic experiments have provided an important confirmation of this model and will compare the results obtained by these authors concerning $\text{NaF}:\text{Cu}^+$ with ours by careful analysis of the temperature dependence of the emission lifetime.

II. EXPERIMENTAL

The crystals investigated in the study and those used in previous works^{1,2} were extracted from the same boules. They were grown via a Bridgman technique and doped

with CuI or CuF_2 . The typical concentration of Cu^+ in the NaF crystals is around 200 ppm. The fluorescence was excited with a pulsed dye laser pumped with a neodymium:yttrium-aluminum-garnet (Nd + YAG) laser and followed by a wavelength extender which allows one to work up to 2230 Å. The sample was placed in a cryostat allowing work in the temperature range 1.5–300 K. The fluorescence was detected through the slits of a Hilger and Watts monochromator (Monospek model No. 1000) (band path 1–2 Å) by an EMI model No. 6256 S photomultiplier tube. The signal was amplified, discriminated, and shaped by a photon-counting system and sent to the same data-acquisition and control system as previously described.⁴

III. RESULTS AND DISCUSSION

The fluorescence decays were obtained by exciting in the absorption band at 3100 Å which was assigned to the 1E_g excited state.^{1,2} The decays are purely exponential over the range of temperature investigated, i.e., between 2 and 300 K. They do not depend on the part of the emission spectrum which is observed. It should be noted that the emission spectrum exhibits two peaks, at 3750 and 3950 Å above room temperature, which coalesce and shift to 3700 Å at 77 K. The double-humped band could be a manifestation of a dynamic Jahn-Teller effect on the 3E_g excited state similar to that clearly established on the 1E_g state by one- and two-photon absorption measurements.² The decays, for each temperature, were recorded systematically for three emission wavelengths: 3600, 3700, and 4100 Å corresponding to the wings and the center of the emission spectrum, excepted in the range of high temperatures ($T > 250$ K where the two peaks appear), for which many data points were obtained between 3600 and 4100 Å. The data obtained were the same within a few percent which correspond to the error of the measurements. Therefore, it seems that, under the hypothesis of the existence of a dynamic Jahn-Teller effect, the kinetics of the emission process which could occur from the two groups of minima of the adiabatic potential excited state are quite similar.

The temperature dependence of the decays is represent-

ed in Fig. 1. One notes the very large increase of the time constant τ when the temperature decreases since τ varies from around $95 \mu\text{s}$ at room temperature to $1474 \mu\text{s}$ at $T=2 \text{ K}$. This variation is very different according to the temperature range. At very low temperatures, $T \leq 5 \text{ K}$, the curve shows a plateau where τ has a constant value, while at $5 < T < 50 \text{ K}$, τ is strongly temperature dependent [Fig. 1(a)]. For temperatures greater than 50 K , the time constant decreases very slowly: $\tau=150 \mu\text{s}$ at $T=60 \text{ K}$ and $\tau=95 \mu\text{s}$ at $T=300 \text{ K}$ [Fig. 1(b)].

We now examine the various sources of temperature dependence of τ . A radiationless process from emitting levels is a possible cause of T dependence of τ , but in the case of Cu^+ , the emission never quenches at temperature less than 300 K , and thus its effect on the observed lifetimes must be ruled out. The fluorescent emission is a vibrationally allowed transition, and therefore, a decrease of τ with rising temperature is expected. The vibronic coupling effects were studied in detail by Payne *et al.*² by using one- and two-photon spectroscopy. They have measured, in the ${}^1T_{1g}$ and 1E_g states, the frequencies of the t_{1u} enabling mode which induces the transition moment in the one-photon spectrum. The one-quantum frequency $\hbar\omega$ of the t_{1u} mode in the 1E_g state was found to be equal to 17.5 cm^{-1} . This value can be extrapolated to the 3E_g states which are close to the 1E_g singlet state. In the simple case of a linear electron-phonon interaction, the temperature dependence of τ due to this vibronic coupling should be fitted by the relation

$$\frac{1}{\tau} = \frac{1}{\tau_0} \coth \frac{\hbar\omega}{2kT} \quad (1)$$

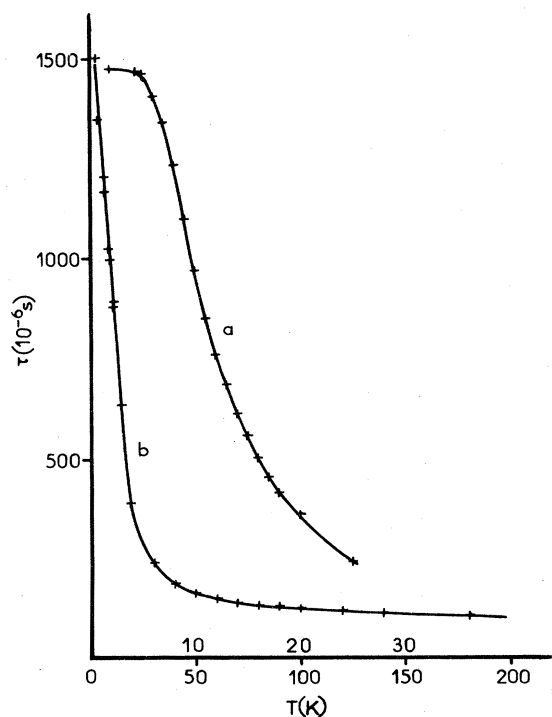


FIG. 1. Temperature dependence of the decay of fluorescent emission (at about 3800 \AA) excited in the 1E_g excited state (3100 \AA) of NaF:Cu^+ . Curves *a* and *b* refer to the upper scale and the lower scale, respectively.

Figure 2 represents a plot of the experimental data of $\tau(0)/\tau(T)$ and calculated values deduced from Eq. (1) for $\hbar\omega=17.5$ and 35 cm^{-1} [one-quantum frequencies deduced from the (0-1), (0-2), and (0-3) lines²]. It is clear that the relation (1) cannot account for the experimental results. In fact, the contribution of the vibronic coupling to the T dependence of τ is very difficult to evaluate because the potential of the 1E_g state was found to be strongly anharmonic and a strong Jahn-Teller distortion exists in this state.² However, it is difficult to imagine that the introduction of a quadratic term⁸ or the use of more than one frequency in Eq. (1)^{9,10} could fit the experimental results. The contribution of the phonons to the T dependence of τ is probably much weaker than those which are mainly responsible for the observed variation, that is to say, the splitting of the 3E_g emitting state into the T_{1g} and T_{2g} spin-orbit components. Consequently, in the following, only this last contribution will be considered.

The model that we propose to describe the kinetics of fluorescence is the same model we have already successfully used for other compounds doped with Cu^+ and Ag^+ ions.³⁻⁶ The emitting levels are the two spin-orbit components T_{1g} and T_{2g} of the metastable 3E_g state, which is the lowest state in the d^9s manifold. Multiple scattering $X\alpha$ ($\text{MSX}\alpha$) calculations^{11,12} have shown that the energies of these states are very close, so that thermal equilibrium is rapidly achieved when a photon is absorbed directly in these states (but the probability is very weak) or in the higher 1E_g singlet state after a fast relaxation into the emitting levels. The spin-orbit coupling can mix $T_{2g}({}^3E_g)$ with T_{1g} , and as a result T_{2g} acquires a significant singlet character (1-2%), while the $T_{1g}({}^3E_g)$ level cannot interact with the singlets of the $3d^94s$ electronic configuration. The emission rate of the lowest $T_{1g}({}^3E_g)$ excited state is therefore much weaker than that of the $T_{2g}({}^3E_g)$ state. Consequently, the fluorescence decays can be interpreted by a three-level system (Fig. 3) consisting of the ground state ${}^1A_{1g}$ (level 1) and two close thermalized metastable excited states (levels 2 and 3), the lifetime of the lowest one (level 3) being much longer than the upper one (level 2). It should be noted that a fourth level (singlet

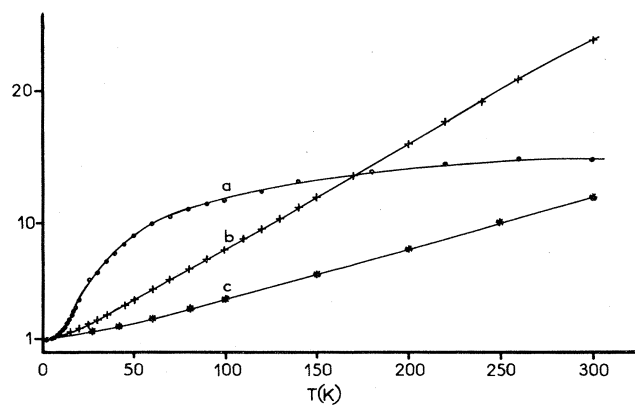


FIG. 2. Curve *a*, $\tau(0)/\tau(T)=f(T)$; curve *b*, $\coth(\hbar\omega/2kT)=f(T)$ with $\hbar\omega=17.5 \text{ cm}^{-1}$; and curve *c*, $\coth(\hbar\omega/2kT)=f(T)$ with $\hbar\omega=35 \text{ cm}^{-1}$.

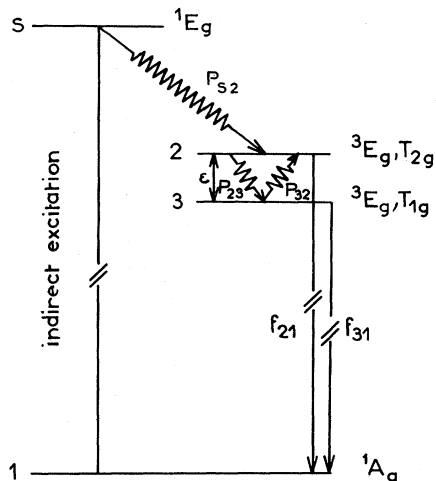


FIG. 3. Three-level model for the emission process.

1E_g) is indicated in Fig. 3 because it is the state in which the electron is directly excited by laser excitation. However, it is not involved in the emission process observed. This is due to the fact that p_{s2} is sufficiently large to consider, after a very short time, the singlet level is empty, level 2 is populated, and the observation starts only then. Hence, the emission process occurs as if level 2 was directly excited.

We call A_{ij} the radiative probability, p_{ij} the radiationless probability, and $f_{ij} = A_{ij} + p_{ij}$ between two i and j levels. In the temperature range of interest, $f_{21} = A_{21}$ and $f_{31} = A_{31}$ since, as mentioned above, the fluorescence-quenching temperature greatly exceeds room temperature. The general solution of the dynamical equations for a three-level system is easily obtained by using Laplace transforms of the level populations (see, for example, Refs. 13–15).

By solving the appropriate rate equations, two time constants τ_s (slow component) and τ_f (fast component) are obtained,

$$\tau_s^{-1} = \frac{1}{2}(\alpha + \beta) + \frac{1}{2}[(\alpha + \beta)^2 - 4(\alpha\beta - p_{32}p_{23})]^{1/2}, \quad (2)$$

$$\tau_f^{-1} = \frac{1}{2}(\alpha + \beta) - \frac{1}{2}[(\alpha + \beta)^2 - 4(\alpha\beta - p_{32}p_{23})]^{1/2}, \quad (3)$$

with

$$\alpha = p_{32} + A_{31}, \quad (4)$$

$$\beta = p_{23} + A_{21}. \quad (5)$$

In order to obtain tractable relations, we introduce the simplifying approximation

$$A_{21}, A_{31} \ll p_{23}, p_{32}, \quad (6)$$

which is often met in practice. In this case, two approximate time constants are obtained,

$$\tau_s^{-1} \approx \frac{A_{31}p_{23} + A_{21}p_{32}}{p_{23} + p_{32}}, \quad (7)$$

$$\tau_f^{-1} \approx p_{23} + p_{32}. \quad (8)$$

We focus our attention first on the long-lived com-

ponent. With levels 2 and 3 existing in thermal equilibrium, we have

$$p_{32} = p_{23} \exp(-\epsilon/kT), \quad (9)$$

where ϵ represents the energy mismatch between the two excited states. If follows that relation (7) reduces to

$$\tau_s^{-1} \approx \frac{A_{31} + A_{21} \exp(-\epsilon/kT)}{1 + \exp(-\epsilon/kT)}. \quad (10)$$

Since the lowest sublevel T_{1g} is exclusively populated at very low temperature, A_{31} is simply the inverse of the observed lifetime and is found to be 678 s^{-1} . Therefore knowing A_{31} , we have fitted our experimental data in the range $6 \leq T \leq 300 \text{ K}$ with the expression (10) with two parameters A_{21} and ϵ . We obtained a very good fit for $\epsilon = 27.2 \text{ cm}^{-1}$ and $A_{21} = 17322 \text{ s}^{-1}$, as can be seen in Fig. 4. The value of A_{21} is close to that which is approximately estimated in many cases from the lifetime at room temperature,⁷

$$A_{21} \approx \frac{2}{\tau(300 \text{ K})} \approx 21000 \text{ s}^{-1}. \quad (11)$$

It should be noted that the approximation (6) may not be well verified at very low temperatures, where p_{32} is strongly slowing down according to relation (9). Then it is possible to introduce the following approximations:

$$A_{21} \gg A_{31}, \quad p_{23} \gg p_{32}.$$

Thus,

$$A_{21} + p_{23} \gg A_{31} + p_{32}. \quad (12)$$

We then obtain for the slow component

$$\tau_s^{-1} \approx A_{31} + (A_{21}p_{23})/(p_{23} + A_{21}). \quad (13)$$

It follows from Eq. (9) that

$$\tau_s^{-1} \approx A_{31} + (1/A_{21} + 1/p_{23})^{-1} \exp(-\epsilon/kT). \quad (14)$$

This last relation is very well verified for $T \ll 12 \text{ K}$ (Fig. 5). A linear dependence of $\ln(1/\tau_s - A_{31})$ on $1/T$ is

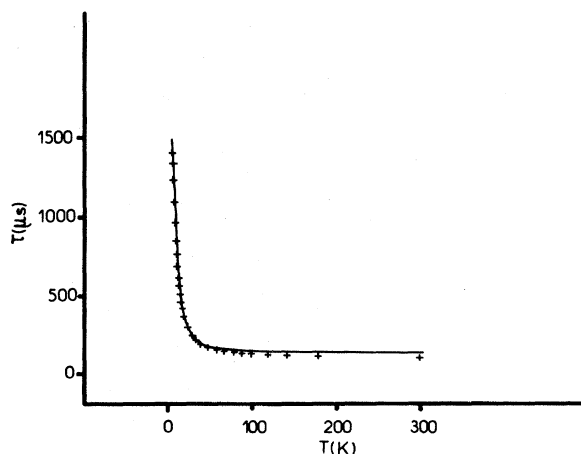


FIG. 4. Experimental time constant τ versus temperature T . The solid line represents the best fit with relation (10) (see text) obtained with $\epsilon = 27.2 \text{ cm}^{-1}$ and $A_{21} = 17322 \text{ s}^{-1}$.

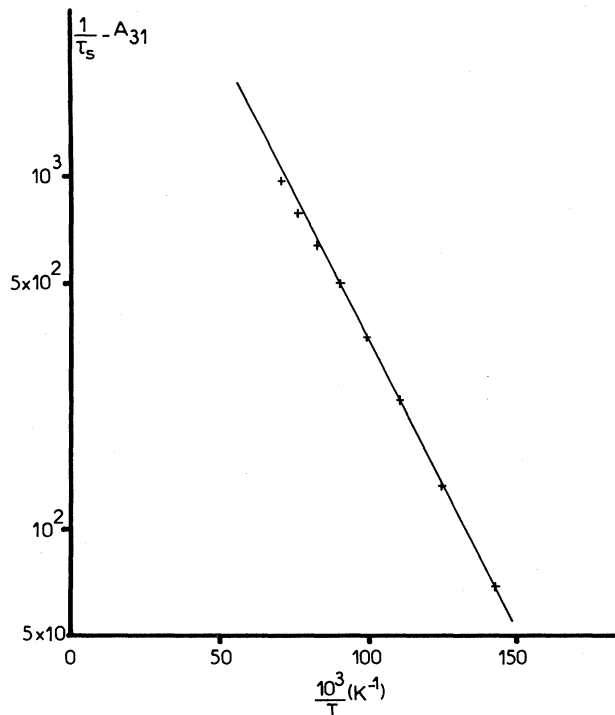


FIG. 5. Temperature dependence of the slow component τ_s in the very low-temperature range ($T \leq 14$ K). The experimental points are fitted with the function

$$\ln(1/\tau_s - A_{31}) = \ln[(1/A_{21} + 1/p_{23})^{-1}] - (\epsilon/k)(1/T),$$

with $A_{31} = 678 \text{ s}^{-1}$.

obtained, and the measurement of the slope of the straight line gives $\epsilon \approx 26.7 \text{ cm}^{-1}$, a value very close to that deduced from relation (10), indicating a good coherence of the approximations (6) and (12) valuable for different ranges of temperature.

The difference between the emission probabilities A_{21} and A_{31} of $T_{2g}(^3E_g)$ and $T_{1g}(^3E_g)$, respectively, should be exclusively due to the mixing of the singlet state $^1T_{2g}$ into the $T_{2g}(^3E_g)$ state, since it is reasonable to admit that these sublevels would have the same lifetime if they had 0% singlet states in them. Thus, it is interesting to check if, for the given value of $A_{31} = 678 \text{ s}^{-1}$, the value of $A_{21} = 17300 \text{ s}^{-1}$ is the value that was expected from theory. The contribution of the singlet-triplet mixing to the increase of the emission probability is therefore about the difference between A_{21} and A_{31} , i.e., approximately 16600 s^{-1} . Like Payne *et al.*⁷ we use the following relation to relate the lifetime of the 3E_g state, τ_t , to its oscillator strength f_t and the emission band energy ν :

$$f_t = \frac{1.5}{\nu^2(\text{cm}^{-1})\tau_t(\text{s})} = \frac{1.5A_{21}}{\nu^2}. \quad (15)$$

The absorption band corresponding to the $^1A_{1g} \rightarrow ^3E_g$ transition is too weak to be observed, and thus f_t cannot be measured experimentally. However, the wave function of the $T_{2g}(^3E_g)$ state can be written as a linear combination of the $^1T_{2g}$, $^3T_{2g}$, and 3E_g states which are mixed by

the spin-orbit coupling.¹¹ Thus,

$$|T_{2g}(^3E_g)\rangle = C_s |^1T_{2g}\rangle + C_{t1} |^3E_g\rangle + C_{t2} |^3T_{2g}\rangle. \quad (16)$$

It is found that

$$f_t = |C_s|^2 f_s, \quad (17)$$

where f_s represents the oscillator strength of the singlet $^1T_{2g}$ state. Relations (15) and (17) lead to

$$A_{21} = \frac{|C_s|^2 \nu^2}{1.5} f_s. \quad (18)$$

The value of the oscillator strength f_s at 2 K is about 10^{-3} , while ν is found to be near 27000 cm^{-1} at $T = 4.4$ K. With $A_{21} \approx 17300 \text{ s}^{-1}$, relation (18) leads to $|C_s|^2 \approx 3.5\%$. To be more precise, the difference of $A_{21} - A_{31}$ should be considered instead of A_{21} in Eq. (18), but this minor correction leads to a similar result, i.e., $|C_s|^2 \approx 3.4\%$. This value is comparable to 1.8% obtained on the NaCl:Cu⁺ system from MSX α calculations.¹² The larger mixing deduced for NaF:Cu⁺ is quite logical since the energy difference between the $T_{2g}(^3E_g)$ state and the singlet $^1T_{2g}$ state [with which the first state is mixed (by spin-orbit coupling)] is smaller in this system. The good agreement between theory and experiment strongly supports our two-state theory of emission.

Another important confirmation of our model was brought about by Payne *et al.*⁷ They had the excellent idea to utilize an external magnetic field to mix the spin-orbit levels. They observed a measurable decrease in the emission lifetime of the T_{1g} sublevel which gains significant singlet character from the mixing with $T_{2g}(^3E_g)$. They were able to analyze quantitatively the magnetic field effect on the emission process, and calculated the T_{1g}, T_{2g} spin-orbit splitting. They obtained very good agreement with our results since they found $\epsilon = 26 \text{ cm}^{-1}$ compared to the value $\epsilon = 27 \text{ cm}^{-1}$ which we found from our analysis of the kinetics of the emission process as a function of temperature.

We now consider the short-lived component τ_f . It is not always easily observed, depending on the relative value of its time constant compared to that of τ_s , and the temperature dependence of its quantum yield, which often strongly decreases with rising temperature.¹⁶ In the present case we have not seen τ_f , probably because it is too short to be detected with our multichannel scaling data-acquisition mode (with a minimum dwell time per channel equal to $2 \mu\text{s}$). Actually, relation (8) gives $\tau_f^{-1} \approx p_{23} + p_{32} \approx p_{23}$ at low temperature. One can deduce the value of p_{23} from relation (14). Owing to the fact that the intercept at the ordinate axis is very sensitive to the weakest variation of the slope of the straight line, one can obtain only an order of magnitude for p_{23} . One finds $p_{23} > 10^6 \text{ s}^{-1}$, and thus τ_f is expected to be shorter than $1 \mu\text{s}$. We are now ready to consider the future investigation of the very-short-time range after the excitation pulse with another setup for lifetime measurements.

In conclusion it can be said that the model we have proposed in the last few years to describe the emission process in Cu⁺ and Ag⁺ impurity centers introduced in some

alkali halides is also valid in the present system, NaF:Cu⁺. Experiment and theory are particularly in very good agreement in this case, where the Cu⁺ impurity is really in an on-center position. Lifetime measurements allowed us to evaluate, with good accuracy, the values of the various parameters which are involved in the kinetics of fluorescence, such as the energy difference ϵ between the two emitting sublevels of the 3E_g state, and the emission probabilities of the excited states; direct spectroscopy

methods, such as absorption measurements, are not able to elucidate any more information because of the very weak transition probabilities of emitting levels.

ACKNOWLEDGMENTS

We wish to thank Dr. Stephen A. Payne and Professor Donald S. McClure, who have sent us their latest results (Ref. 7), and for many helpful discussions.

-
- ¹A. B. Goldberg, D. S. McClure, and C. Pedrini, *Chem. Phys. Lett.* **87**, 508 (1982).
²S. A. Payne, A. B. Goldberg, and D. S. McClure, *J. Chem. Phys.* **78**, 3688 (1983).
³C. Pedrini, *Phys. Status Solidi B* **87**, 273 (1978).
⁴C. Pedrini, *J. Phys. Chem. Solids* **41**, 653 (1980).
⁵C. Pedrini and B. Jacquier, *J. Phys. C* **13**, 4791 (1980).
⁶C. Pedrini, *Solid State Commun.* **38**, 1237 (1981).
⁷S. A. Payne, R. H. Austin, and D. S. McClure, *Phys. Rev. B* **29**, 32 (1984).
⁸K. Fussgänger, *Phys. Status Solidi* **36**, 645 (1969).
⁹K. Fussgänger, W. Martienssen, and H. Bilz, *Phys. Status Solidi* **12**, 383 (1965).
¹⁰C. Pedrini, H. Chermette, A. B. Goldberg, D. S. McClure, and B. Moine, *Phys. Status Solidi B* **120**, 753 (1983).
¹¹H. Chermette and C. Pedrini, *J. Chem. Phys.* **75**, 1869 (1981).
¹²H. Chermette and C. Pedrini, *J. Chem. Phys.* **77**, 2460 (1982).
¹³B. I. Stepanov and V. P. Gribkovskii, *Theory of Luminescence* (ILIFFE, London, 1968), p. 438.
¹⁴B. Di Bartolo, *Optical Interactions in Solids* (Wiley, New York, 1968), p. 437.
¹⁵G. Boulon, C. Pedrini, M. Guidoni, and Ch. Pannel, *J. Phys. (Paris)* **36**, 267 (1975).
¹⁶M. F. Trinkler, I. K. Plyavin, B. Y. Berzin, and A. K. Everte, *Opt. Spectrosk.* **16**, 378 (1964) [*Opt. Spectrosc. (USSR)* **19**, 213 (1965)].